17th World Conference on Earthquake Engineering, 17WCEE
Sendai, Japan - September 13th to 18th 2020
Paper N° C004014
Registration Code: S-A02327

SEISMIC LOSS ASSESSMENT OF HIGHWAY BRIDGES FOR DIFFERENT AZIMUTHS OF GROUND MOTIONS

Anastasios Sextos[(1)], Ruiwei Feng[(2)], Wancheng Yuan[(3)]

[(1)] *Professor, Department of Civil Engineering, University of Bristol, a.sextos@bristol.ac.uk*
[(2)] *Ph.D. Candidate, State Key Laboratory of Disaster Reduction in Civil Engineering, Tongji University, rwfeng@tongji.edu.cn*
[(3)] *Professor, State Key Laboratory of Disaster Reduction in Civil Engineering, Tongji University, yuan@tongji.edu.cn*

Abstract

Previous studies have highlighted the difficulty of identifying the critical seismic incidence angle in terms of the resulting response at both the structure and the component level. An inherent complexity of this problem is that the critical angle depends on the characteristics of input ground motion itself, while it varies for each different structural component. This observation hinders the development of guidelines for seismic design and assessment of structures, especially for those which have relatively complicated configurations. To address this issue, this study aims to examine the problem from a different perspective by probabilistically assessing the influence of ground motion azimuth on the overall seismic monetary loss of the structural system. An already constructed, 638-m-long, twelve-span prestressed concrete curved highway bridge was adopted as the bridge example. Nonlinear response history analyses (NRHA) were implemented using a set of real ground motion records along different incidence angles. Several intensity measures (IM) were comparatively assessed including a number of newly introduced ones and the most efficient IM was adopted considering the contributions of higher modes to the structural response. The superiority of the latter was validated by comparing the results with other commonly used IM candidates based on the existing evaluation criteria. Finally, multidirectional seismic loss estimates were conducted, and the variability of the total repair cost with respect to the excitation direction and the ground motion intensity was derived. Results indicate that considering the contribution of higher modes in defining an IM is conducive to predict the probabilistic seismic demand of a curved bridge. There is probably an underestimation for the real seismic loss if the horizontal orthogonal ground motion components are only applied along the principal axes of the bridge, without due consideration of seismic excitation direction. Most importantly, the impact of seismic incidence angle gradually becomes less significant with increasing level of ground motion intensity and damage throughout the bridge system. This practically implies that potential rules for considering the directionality of earthquake input shall be consistent with the respective limit state examined.

Keywords: Loss estimation; seismic excitation direction; curved bridge; seismic intensity measure

1. Introduction

In the past fifty years, disastrous seismic events happened in different parts of the world. As one of the most important transportation hubs in lifeline engineering, bridges suffered from severe damage during earthquakes. Plenty of researchers studied the effect of earthquake characteristics on the dynamic response of buildings and bridges [1–3]. The ground motions parameters considered in above studies mainly include frequency content, duration, and pulse-like velocity component. However, the angle of seismic incidence, which is highly random, has been proven to have significant design implications on buildings [4], as well as a non-negligible impact on bridges [5], is only rarely investigated. Particularly for curved bridges, which have more complex seismic behavior due to their curvature in plan and the large number of modes contributing, previous studies (e.g. [6]) have shown that the effect of ground motion incidence angle may modify the seismic demand by up to 80%. Several other studies have recently focused on the seismic performance of curved bridges considering different azimuths of ground motions [7,8] leading to methods for determining their critical angles of seismic incidence [9,10] at component level. What is commonly observed (e.g. [5,7,11]) is that: (a) the critical orientation varies for different Engineering Demand Parameters (EDP) under the same excitation and (b) that different earthquake records may lead to clearly different critical angles even for the same EDP examined. These findings highlight the difficulty associated with identifying in a reliable way the critical direction for a bridge system by means of individual ground motion records and EDPs. As a result, there is a need for alternative criteria at a lower resolution of assessment.

Performance-based earthquake engineering (PBEE) provides an effective approach for probabilistically assessing the system performance of a bridge. Along these lines, downtime and monetary loss are the two main evaluation criteria in this framework. Over the last two decades, several studies have been devoted to the loss assessment method of bridges, by means of incremental dynamic analysis [12] neural networks [13], as well as considering the effects of aging [14] and loss of functionality [15]. However, only a few of them focus on curved bridges when assessing the direction dependent variability of total bridge loss.

Given the significance of ground motion directionality in the seismic response assessment of curved bridges and the existing limitations in current methods for determining the critical angle of seismic incidence, this study conducted a seismic loss assessment for a well-studied curved bridge with particular emphasis on the effects of seismic excitation direction. The direct total repair costs of the bridge system were adopted as the decisive criterion for the performance of the bridge system, and a multi-directional probabilistic loss assessment method was developed. The numerical model of a 638 m long, twelve-span curved continuous prestressed concrete bridge was established and 2,400 (100 ground motion pairs × 24 incidence angles) nonlinear response history analyses (NRHA) were performed. Based on the results of NRHA, an IM considering the contribution of higher modes was further proposed and its optimal behavior for the probabilistic demand analysis of curved bridges was validated. The details of the methodology, case study and results are discussed in the following sections.

2. Methodology

The loss assessment method adopted is an extension of that proposed by Kameshawar and Padgett's [13], which considers the effects of different angles of seismic incidence. In order to incorporate the uncertainty in assessing the damage state of the bridge component, for the bridge subjected to k^{th} ground motion pair (GM_k) along the j^{th} excitation direction, N_{mc} (1×10^5) Monte Carlo simulations (MCSs) were implemented. In terms of the i^{th} MCS, the total repair cost of the bridge system, $C_t^i\,(GM_k,\theta_j)$, can be written as:

$$C_t^i\,(GM_k,\theta_j)= \sum_{c=1}^{n_c} C_c^i(GM_k,\theta_j)\ , \tag{1}$$

where n_c is the number of different structural component types that are taken into account in the loss assessment. In this study piers, bearings and abutments were involved assuming that the bridge deck remains elastic during seismic motion, therefore $n_c = 3$. C_c^i is the overall repair cost for component type c, which consists of the repair cost of its damage mode d ($C_{d|c}^i(GM_k,\theta_j)$) and can be calculated as:

$$C_c^i\,(GM_k,\theta_j)= \sum_{d=1}^{n_{d|c}} C_{d|c}^i(GM_k,\theta_j)\ , \tag{2}$$

where $n_{d|c}$ is the number of damage modes that can be used to represent the performance of the respective component. In the current study, the damage of the bearing is described by the shear strain, the abutment damage is due to its active and passive response, while the pier damage is accounted for the maximum curvature ductility of its bottom section for both tangent and radial directions. The $C^i_{d|c}(GM_k,\theta_j)$ is then the sum of the cost for all the elements belonging to component c that experience damage mode d ($C^i_{e|d|c}(GM_k,\theta_j)$) and is expressed as:

$$C^i_{d|c}(GM_k,\theta_j)= \sum_{e=1}^{n_{e|d|c}} C^i_{e|d|c}(GM_k,\theta_j)\ , \tag{3}$$

where $n_{e|d|c}$ is the total number of elements. It is worth noting that the $C^i_{e|d|c}(GM_k,\theta_j)$ depends on the damage state ($DS^i_{e|d|c}(GM_k,\theta_j)$) of the element e, which can be given as:

$$DS^i_{e|d|c}(GM_k,\theta_j) = \sum_{l=1}^{4} I\,(D^i_{e|d|c}(GM_k,\theta_j) > S^i_{l|e|d|c}(GM_k,\theta_j)), \tag{4}$$

in which:

$$I\,(\cdot) = \begin{cases} 1 & D^i_{e|d|c}(GM_k,\theta_j) \ \geq \ S^i_{l|e|d|c}(GM_k,\theta_j) \\ 0 & D^i_{e|d|c}(GM_k,\theta_j) \ < \ S^i_{l|e|d|c}(GM_k,\theta_j) \end{cases}. \tag{5}$$

In Eq. (4), $D^i_{e|d|c}(GM_k,\theta_j)$ and $S^i_{l|e|d|c}(GM_k,\theta_j)$ are the demand and capacity (in damage state l) of element e, respectively. It assumes that the $S^i_{l|e|d|c}(GM_k,\theta_j)$ follows a two-parameter lognormal distribution and is generated by the median S_c and dispersion β_c, which can be seen in Table 1. In Eq. (5), $I\,(\cdot)$ is the indicator function to identify the inequal relationship between $D^i_{e|d|c}(GM_k,\theta_j)$ and $S^i_{l|e|d|c}(GM_k,\theta_j)$. A total of five alternative values (i.e. 0,1,2,3,4) are provided for $DS^i_{e|d|c}(GM_k,\theta_j)$, which corresponds to no damage, slight damage, moderate damage, extensive damage and complete damage, respectively. Once the $DS^i_{e|d|c}(GM_k,\theta_j)$ is determined, the $C^i_{e|d|c}(GM_k,\theta_j)$ can be predicted as:

$$C^i_{e|d|c}(GM_k,\theta_j) = \sum_{l=1}^{4} \delta\,(l\text{-}DS^i_{e|d|c}(GM_k,\theta_j))\,\overline{C_{l|e|d|c}}, \tag{6}$$

where $\delta\,(\cdot)$ is the Dirac delta function, and $\overline{C_{l|e|d|c}}$ is the average repair cost of element e in damage state l and can be calculated by:

$$\overline{C_{l|e|d|c}} = \sum_{r=1}^{n_{r|d|c}} \overline{C_{r|d|c}} P_{r|l|e|d|c} Q_{r|e|d|c}(X), \tag{7}$$

where $n_{r|d|c}$ is the total number of repair actions for damage mode d of component c, $\overline{C_{r|d|c}}$ is the average unit cost of repair action r, $P_{r|l|d|c}$ is the probability of the selected repair action r for damage state l, and $Q_{r|e|d|c}(X)$ is the quantities of material and dimension that are used for the repair of element e, herein X represents the bridge parameters (e.g. span length, column height and nominal strength of concrete) as well as the average unit costs of the adopted materials. The values for $\overline{C_{r|d|c}}$ and $P_{r|l|d|c}$ can be referred to Kameshawar and Padgett's [13], and $Q_{r|e|d|c}(X)$ can be obtained based on the engineering judgement. Further, Substituting Eqs. (2)-(7) into Eq. (1), the total bridge cost of the i^{th} simulation for ground motion pair k along the incidence angle θ_j becomes:

$$C^i_t\,(GM_k,\theta_j)= \sum_{c=1}^{n_c} \sum_{d=1}^{n_{d|c}} \sum_{e=1}^{n_{e|d|c}} \sum_{l=1}^{4} \sum_{r=1}^{n_{r|d|c}} [\delta\,(l\text{-}DS^i_{e|d|c}(GM_k,\theta_j))\,\overline{C_{r|d|c}} P_{r|l|e|d|c} Q_{r|e|d|c}(X)] \tag{8}$$

Hence, in terms of N_{mc} MCSs and N_{eq} ground motion pairs, the average restoration cost for the incidence angle θ_j, $C_t(\theta_j)$, can be derived as:

$$C_t(\theta_j) = \frac{1}{N_{mc}}\frac{1}{N_{eq}} \sum_{i=1}^{N_{mc}} \sum_{k=1}^{N_{eq}} C^i_t\,(GM_k,\theta_j) \tag{9}$$

Table 1 – Capacity model of EDPs

Component	Slight		Moderate		Extensive		Complete		Ref.
	S_c	β_c	S_c	β_c	S_c	β_c	S_c	β_c	
Pier curvature ductility (μ_ϕ)	1	0.25	2	0.25	4	0.25	7	0.25	[16]
Bearing shear strain (γ_b in %)	100%	0.25	150%	0.25	200%	0.25	250%	0.25	[17]
Abutment-passive (δ_p in mm)	37	0.25	146	0.25	1000	0.25	1000	0.25	[18]
Abutment-active (δ_a in mm)	9.75	0.25	37.9	0.25	77.2	0.25	1000	0.25	[18]

3. Bridge configuration and finite element model

3.1 Description of the Krystallopigi bridge

The Krystallopigi bridge is a 12-span, curved, continuous, reinforced concrete (RC) bridge with a total length (L) of 638 m and a radius (R) of 488 m measured to the centerline of the deck [19]. Fig. 1 shows the configuration of this bridge. The deck is a single-cell box with a depth of 2.8 m and a width of 13 m. Expansion joints with an initial gap of 0.15 m are set between the deck and abutments. The piers have rectangular hollow cross sections which become solid at their tops, and their heights vary from 8.66 m to 24 m. The low damping rubber bearings (LDRBs) are set on the end piers (M1, M2, M3, M9, M10, M11), and allow the deck to move tangentially but restrict it radially. The interior piers are monolithically connected to the deck. Abutment A1 and piers M1-M9 are founded on 1.2 m diameter group of piles, which cross the clay layer (V_s = 250 m/s) up to the level of submerged limestone (V_s = 1800 m/s), pier M10 is supported on the debris layer (V_s = 400 m/s) while pier M11 and abutment A2 are founded on shallow foundations directly built on the limestone outcrop. B45 (characteristic cylinder strength f_{ck} = 35 MPa) concrete is used for the deck while B25 (f_{ck} = 20 MPa) is adopted for the abutments and foundations. The piers employ B35 (f_{ck} = 27.5 MPa) and Bst500s (yield strength f_y = 500 MPa)

3.2 Finite element model

The numerical model of Kristallopigi bridge was built using the computer platform OpenSees [20]. Fig. 2 illustrates the finite element model and the simulation details. The deck is modelled using the elastic beam-column elements with lumped masses calculated based on the cross-section properties assigned to the nodes. The bearings were simulated with zero-length elements and their constitution relationships were defined according to Zhang and Huo's [16]. The piers were modelled using nonlinear beam-column fiber elements, and *Concrete 04* was adopted for the simulation of confined and unconfined concrete, wherein the values of parameters for the *Concrete 04* material can be determined according to Mander et al [21]. Elastic beam-column elements were also employed for modelling the pile caps with their masses assigned to the centroids. Soil-structure interaction was considered using 6 degree-of freedom (DOF) linear springs and their stiffness were obtained based on Mylonakis et al. [22]. The responses of the abutment were captured using zero-length elements with different nonlinear constitutive models in the orthogonal directions according to a previous study [17]. The pounding effect at the expansion joints were modelled via zero-length element with the impact material, which is developed from the Hertz contact model [23]. In addition, uncertainty in the modelling parameters was incorporated using Latin Hypercube sampling (LHS) technique. Table 2 shows the probability distribution of these parameters.

4. Ground motions

Considering that the purpose of this study is to draw some general conclusions regarding the variability of bridge loss to the angle of seismic incidence rather than the assessment of a specific bridge, the available seismic hazard disaggregation associated with the bridge site was not used. In contrast, a wider, unbiased sample of 100 ground motion records was selected from NGA-West2 (https://ngawest2.berkeley.edu/) using the unconditional spectrum method [27]. The criteria for the ground motion selection are shown in Table 3. Figure 3 illustrates the acceleration response spectra of the horizontal orthogonal components (EQ_x and EQ_y) of the 100 earthquake records along with their mean values.

Table 2 – Probability distributions of modelling parameters

Modelling parameter	Units	Probability distribution	Ref.
Steel strength	MPa	Lognormal (mean = 6.21, COV = 0.080)	[5]
Concrete strength	MPa	Normal (mean = 27.5, COV = 4.3)	[24]
Bearing shear modulus	MPa	Uniform (lower = 0.702, upper = 1.098)	[25]
Abutment stiffness-passive	kN/mm/m	Normal (mean = 20.2, COV = 3.03)	[26]
Abutment stiffness-active	kN/mm/pile	Normal (mean = 7, COV = 1.05)	[26]
Shear modulus	GPa	Normal (mean = as defined for every pier foundation and for every DOF based on formulae [22], COV = 0.2)	[25]

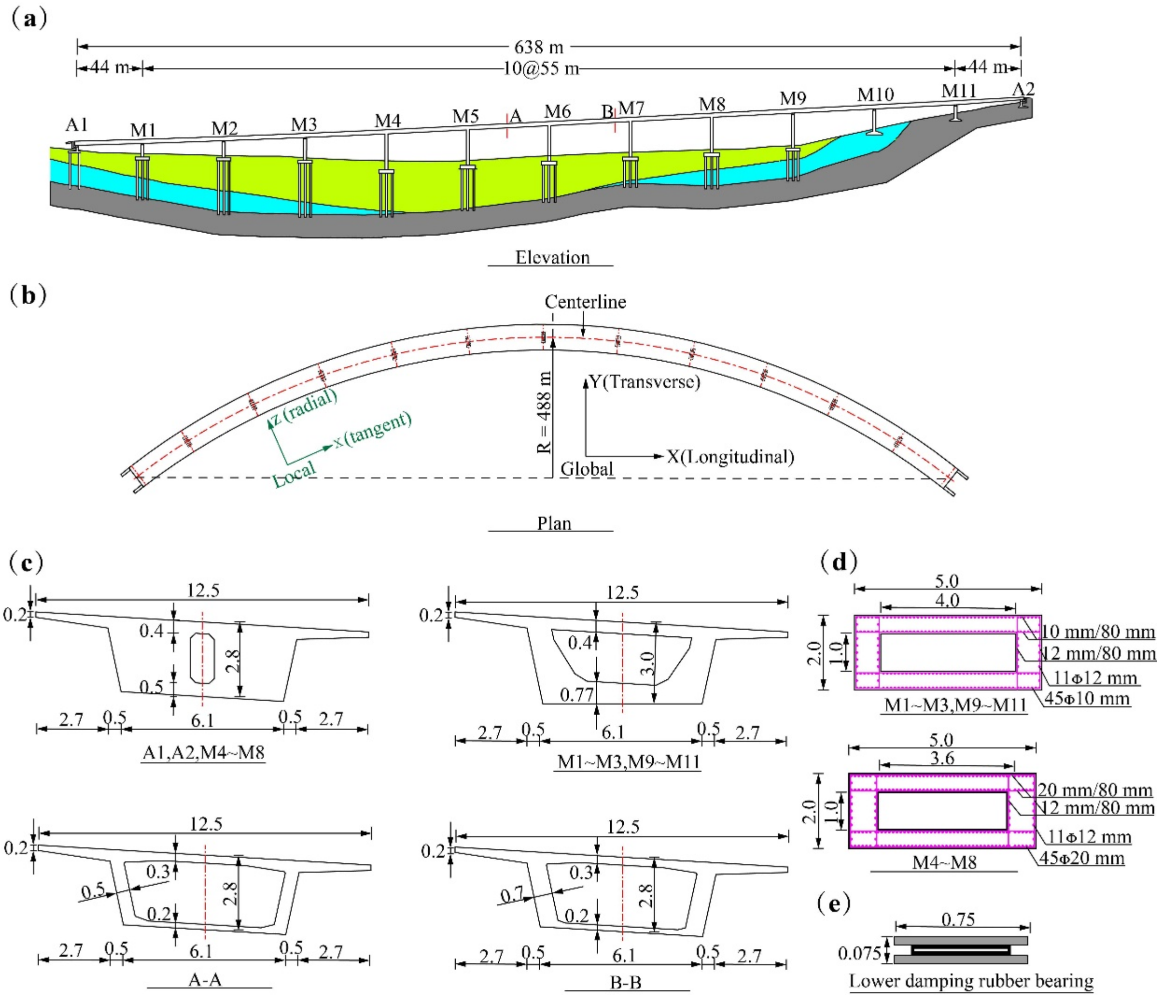

Fig. 1 – Geometric parameters of Krystallopigi Bridge (units: m): (a) elevation, (b) plan, (c) girder section, (d) pier section, (e) bearing

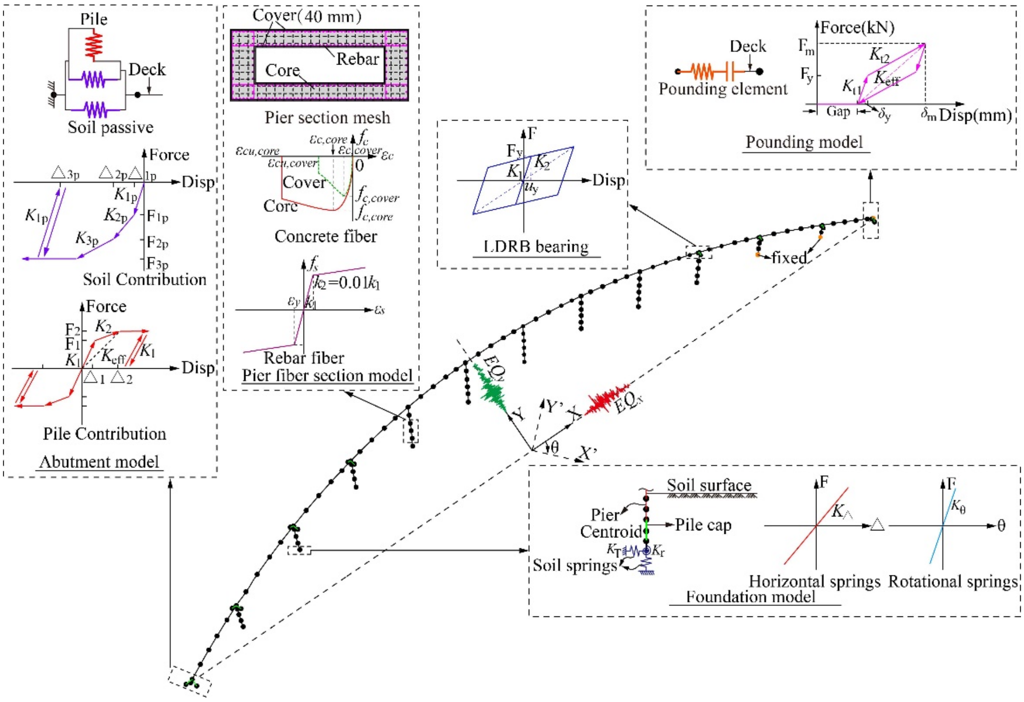

Fig. 2 – Finite element model of Krystallopigi Bridge

Table 3 – Criteria for the ground motion selection

Criteria	Values
Measures of horizontal ground motion components	RotD50
Spectral period of interest	0.01s - 5s
Earthquake magnitude (M_w)	5.5-7.5
Distance to surface projection of the fault rupture (R_{jb})	10 km-60 km
Average shear wave velocity in the top 30 m of the soil (V_{s30})	538 m/s-938 m/s

To consider the effects of angle of seismic incidence, the horizontal orthogonal components of the ground motion record, EQ_x (maximum component) and EQ_y were first applied along the global X and Y axes, respectively, and then rotated by an angle of θ about Z-axis. As shown in Fig.2, θ denotes the included angle between the EQ_x and the X-axis, and it is taken to be positive in the clockwise direction. Due to the asymmetry of this bridge with respect to the global axes, the rotation was conducted at intervals of 15° between 0-360°.

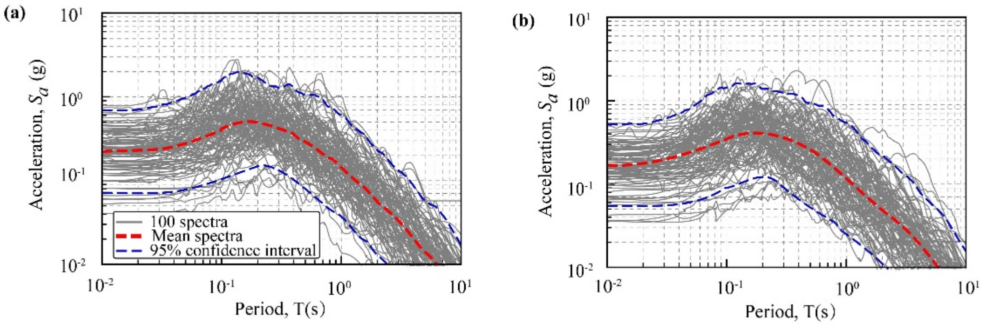

Fig. 3 – Acceleration response spectra of the selected ground motion pairs: (a) EQ_x, (b) EQ_y

5. Probabilistic loss assessment

5.1 Engineering demand parameters

In this study, five engineering demand parameters (EDPs) are selected for the probabilistic loss assessment, namely, peak tangent shear strain of the bearings (γ_b in %), peak tangent ($\mu_{\emptyset_{tt}}, \mu_{\emptyset_{tb}}$) and radial ($\mu_{\emptyset_{rt}}, \mu_{\emptyset_{rb}}$) curvature ductility at the top and the bottom of piers for the case of monolithic pier-deck connections, as well as the peak passive and active abutment displacements (δ_a and δ_p in mm).

5.2 Selection of the optimal IM

A suitable IM can help efficiently predict the probabilistic seismic demands of structures. In recent years, some researchers proposed a few optimum IMs for bridges in different contexts, however few studies aimed at the optimal one for curved bridges. As a fact that higher vibration modes possibly have a non-neglect contribution to the seismic response of curved bridges, two IMs known as the combination of spectral acceleration at critical periods ($S_{a,comb}$) and the combination of spectral displacement at critical periods ($S_{d,comb}$) are proposed herein:

$$S_{a,Comb} = \sqrt{\sum_{k \in M} \alpha_k \left(S_{a,T_k}\right)^2}, \quad S_{d,Comb} = \sqrt{\sum_{k \in M} \alpha_k \left(S_{d,T_k}\right)^2} \tag{10}$$

where M is the set for the number of critical modes, T_k is the period of a significant mode k whose participating mass ratio (α_k) exceeds a threshold taken equal to 30% in this study. For this bridge, the first two vibration modes are critical, thereby $M = \{1,2\}$, and the participating mass ratios are $\alpha_1 = 0.64$ and $\alpha_2 = 0.32$, respectively. Meanwhile, another 8 IMs that are commonly used in probabilistic assessment of curved bridges were selected to comparatively verify the validity of the proposed IMs. Table 4 shows the 10 selected IM candidates, as they were classified into two groups according to their dependency on the specific structures.

Table 4 – Intensity measures selected in this study

IM	Definition	Attribute	IM	Definition	Attribute
PGA	Max$\lvert a(t)\rvert$, $a(t)$ is acc. time history	S-i	$S_{a,10}$	$S_a(\xi=5\%, T=1.0s)$	S-d
PGV	Max$\lvert v(t)\rvert$, $v(t)$ is vel. time history	S-i	S_{d,T_f}	$S_a(\xi=5\%, T=T_f)$	S-d
PGD	Max$\lvert u(t)\rvert$, $u(t)$ is disp. time history	S-i	S_{aC}	$S_a(T_1)\sqrt{\frac{S_a(2T_1)}{S_a(T_1)}}$	S-d
CAV	$\int_0^{t_{tot}} \lvert a(t)\rvert dt$, t_{tot} is the total duration	S-i	$S_{a,Comb}$	$\sqrt{\sum_{k \in M} \alpha_k \left(S_{a,T_k}\right)^2}$	S-d
S_{a,T_f}	$S_a(\xi=5\%, T=T_f)$	S-d	$S_{d,Comb}$	$\sqrt{\sum_{k \in M} \alpha_k \left(S_{d,T_k}\right)^2}$	S-d

*Note: S-i = Structure-independent S-d = Structure-dependent

The criteria for selecting the optimal IM in this study refer to Wang et al. [28], which includes *effeciency*, *proficiency*, *hazard computability*, *practicality*, *sufficiency* and *relative sufficiency*. Given that this study does not involve a specific PSHA the *hazard computability* was not examined in this study. Moreover, the peak values for abutment displacements (δ_a and δ_p), shear strain of outer bearing on abutment A1 (γ_b), and the curvature ductility at the bottom of pier M6 ($\mu_{\emptyset_{tb}}$ and $\mu_{\emptyset_{rb}}$) were used as the representative response quantities of interest. Additionally, the influence of seismic incidence angle on the selection of optimal IM was also considered. For brevity, the results are representatively illustrated for the cases of 0°, 45° and 90°, however, the conclusions are consistent for all the incidence angles. Fig.4 shows the comparative assessment of the IM candidates in terms of the selected EDPs with respect to different angles of seismic incidence. For *efficiency*, *proficiency* and *practicality*, the superiority of an IM is associated with the EDP. Generally, the structure-dependent IMs have higher rankings for the curvature ductility of the pier and the bearing deformation, wherein $S_{a,Comb}$ performs better compared to other fellow candidates; by contrast, the structure-independent IMs have advantages in terms of abutment response, among which *PGV* is the most outstanding one especially for its *practicality*. It is worth noting that *PGD* shows poor behavior for all the EDPs, which indicates that it may not be a satisfactory selection for probabilistic assessment of curved bridges. For *sufficiency*, almost all the IM candidates are sufficient regarding the Magnitude (*M*) while insufficiency (i.e., *p-value* lower than 0.05 in this study) is observed in regard to the epicentral distance (*R*). In particular, all the IMs except the *PGA* show poor *sufficiency* with respect to *R* based on abutment response. In order to determine the relative ranking in terms of *sufficiency* among the IMs, their *relative sufficiency* was obtained. It can be observed that, in general, the structure-dependent IMs are more sufficient than the structure-independent ones, wherein the S_{aC} demonstrates the best one, followed by the S_{a,T_f} and $S_{a,Comb}$. Comparing the results of (absolute) *sufficiency* with those of *relative sufficiency*, it can be seen that they are not consistent with each other, which is actually in accordance with Wang et al. [28]. Besides, similar results for the cases of 0°, 45° and 90° implied that seismic incidence angle has slight effect on the performance of IMs. Overall, although *PGA* is the most commonly-used IM in pobabilistic assessments of both straight and curved bridges, this study shows that it is not be the optimum IM in this case. In short, by comprehensively comparing the results of different criteria involved in this study, $S_{a,Comb}$ was selected as the optimum IM for the following loss estimation sections.

5.2 Multidirectional probabilistic loss assessment

Based on the method outlined in Section 2, the average total bridge loss under every ground motion pair for each angle of seismic incidence was computed. Fig.5 illustrates the results of multidirectional probabilistic loss assessment for different intensities of $S_{a,Comb}$. It can be seen from the figure that the critical angle of seismic incidence is different for different cases of earthquake intensities: $\theta = 195°$ for the case of $0 \leq S_{a,Comb} \leq 0.15$ g, $\theta = 255°$ for $0.15 \text{ g} \leq S_{a,Comb} \leq 0.30$ g, and $\theta = 60°$ is the most critical one for $0.30 \text{ g} \leq S_{a,Comb} \leq 0.60$ g. These results clearly indicate that the critical seismic excitation direction of a curved bridge is associated with the earthquake characteristics and intensity, which is in line with the insights of previous works [5,11]. It can be also inferred that applying the horizontal orthogonal components along the principal axes of curved bridges may underestimate their actual seismic losses. More significantly, it can be seen that the differences among the losses for various seismic incidence angles decrease (maximum gap from 29.4% to 10.3%) as the $S_{a,Comb}$ increases, which demonstrates that the effect of seismic excitation direction on the bridge system weakens with the damage accumulating in the bridge. This observation can be interpreted by the fact the participation of vibration modes is related to the severity of the structural damage. The heavier damage the structure is subjected to, the more significant contribution of higher modes. Moreover, considering the response of a curved bridge is inherently affected by multiple natural modes due to its geometrical shape, it turns out to be less and less sensitive to the direction of seismic excitation as it progresses into the inelastic regime. As a result, the seismic loss eventually becomes direction-independent for the group of strong motions with $S_{a,Comb}$ in the range 0.3 g-0.6 g (Fig. 5(c)).

To visually display the above explanation, time-frequency analyses based on wavelet decomposition were used for representative response parameters in different damage states. For this purpose, the transverse acceleration at the midspan of the deck was adopted as the representative EDP, and two ground motion pairs with different intensities were selected as depicted in Fig. 6. The 1987 Whitter Narrows earthquake (RSN = 594, station = Baldwin Park-N Holly) hereafter known as record #1, causes no damage (and loss), while the 1994 Northridge motion (RSN=1080, station=Simi Valley-Katherine Rd), hereafter called record #2, induces serious damage that leads to an average cost of approximatley $350,000. Fig.7 exhibits the results of time-frequency analyses for both earthquake records. In the time domain, it can be clearly seen from the figure that the transeverse acceleration in the severe damage stage (Fig. 7 (b)) is much larger than the linear-elastic case (Fig. 7 (a)). More notably in the frequency domain, the frequencies that contribute to the bridge response for the case of record #2 are much richer than those under record #1. Specifically, the participation for higher modes is apparent for frequencies between 5.0 Hz and 10.0 Hz, as can be observed for the case of record #2, whereas minor contribution of higher modes is seen in the same frequency range for the case of record #1.

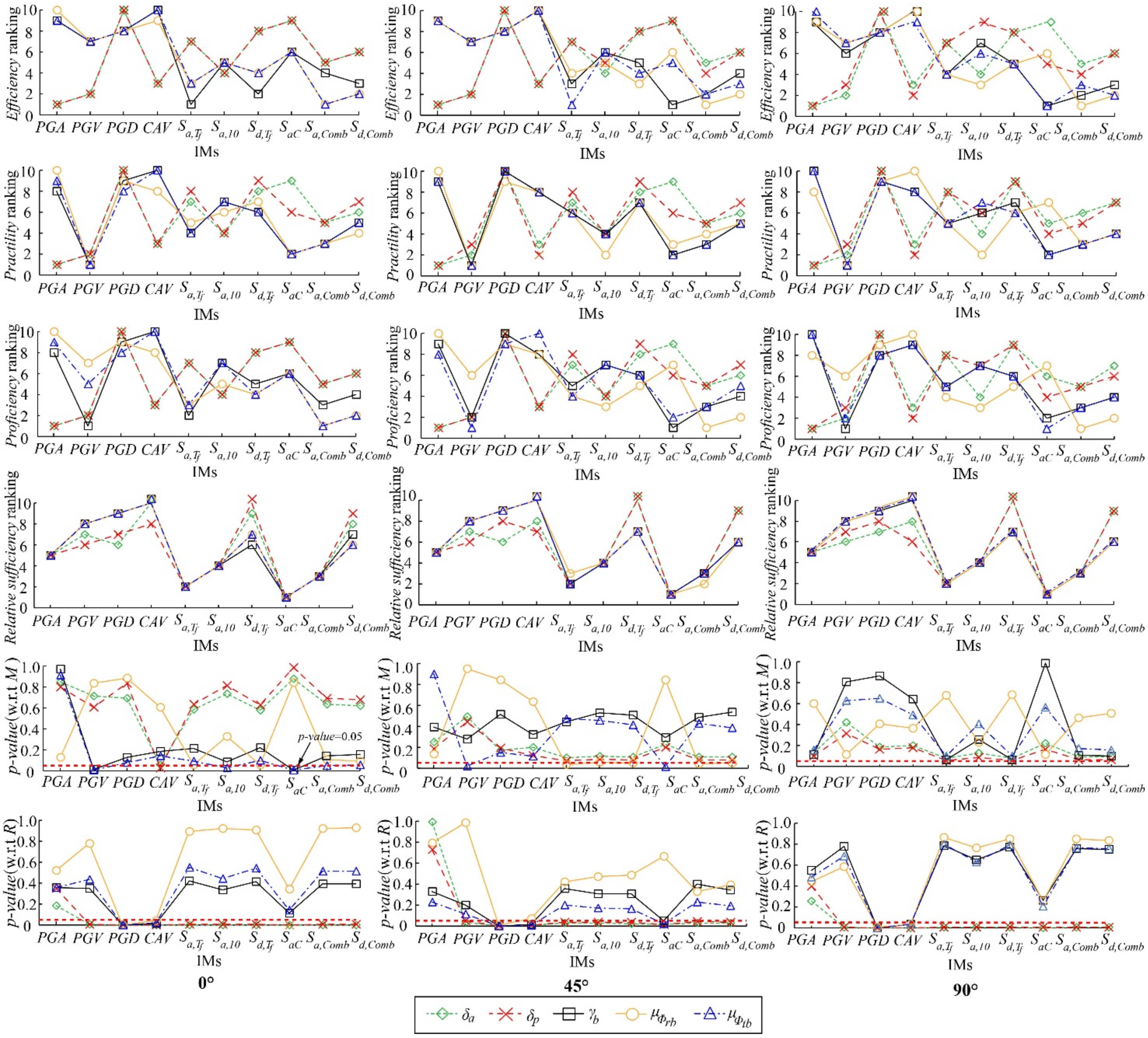

Fig. 4 – Rankings of different IM candidates in terms of *efficiency*, *practility*, *proficiency*, *relative sufficiency* , *sufficiency with respect to magnitude* (*M*) and *sufficiency with respect to epicentral distance* (*R*)

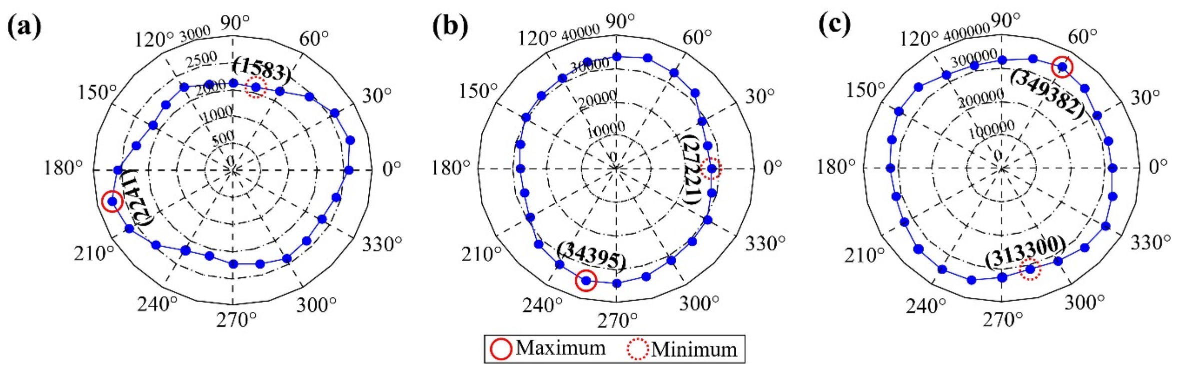

Fig. 5 – Variability of the average repair cost with respect to the seismic incidence angle under the ground motion intensity of: (a) $0 \leq S_{a,Comb} \leq 0.15$ g, (b) 0.15 g $\leq S_{a,Comb} \leq 0.3$ g, and (b) 0.3 g $\leq S_{a,Comb} \leq 0.6$ g

The above indicative results verify that the bridge performance becomes more complex in the nonlinear range and this relates to the impact of ground motion direction. Accordingly, when the bridge is heavily damaged, it simutaneously responds to several different vibration modes hence the angle of seismic incidence becomes marginal.

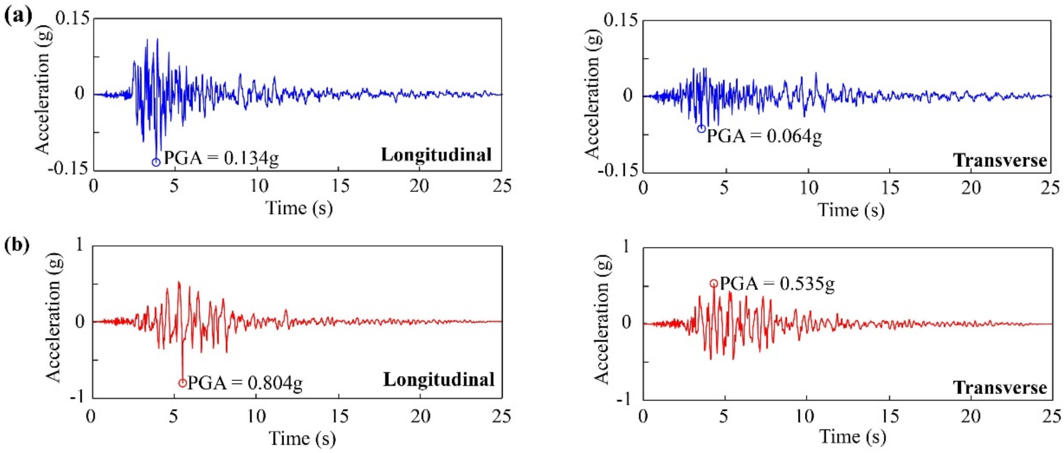

Fig. 6 – Selected ground motion records for the time-frequency analyses: (a) 1987 Whitter Narrows (RSN = 594, station = Baldwin Park-N Holly), (b) 1994 Northridge (RSN=1080, station=Simi Valley-Katherine Rd)

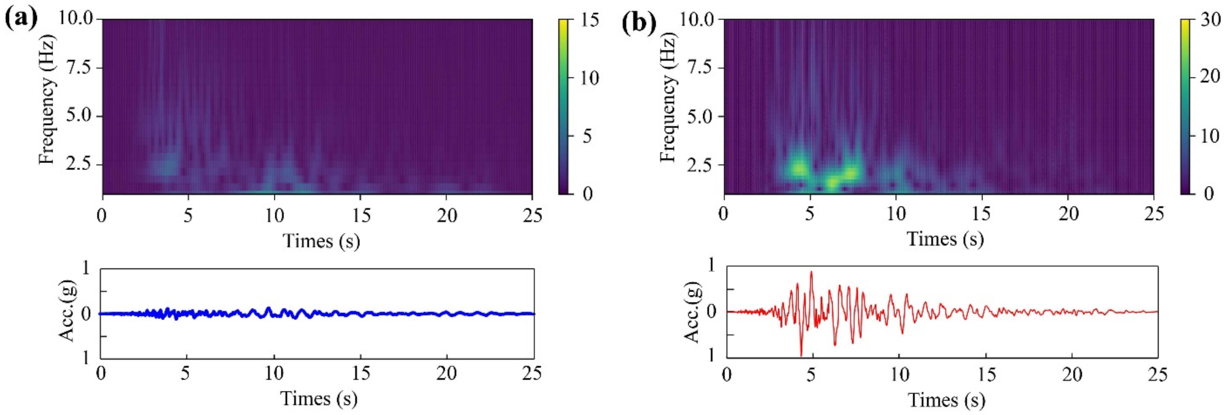

Fig. 7 – Time-frequency analyses of the transverse acceleration at the midspan of the deck for the case of (a) record #1 (Whittier Narrows) motion and (b) record #2 (Northridge) motion

5. Conclusions

This study investigates the effect of seismic incidence angle on the bridge performance using the total moneraty loss as the evaluation criterion. The paper presents the development of a multi-directional probabilistic loss assessment approach based on a previous methodology, the proposal of an IM that better considers the influence of higher natural modes and a comprehensive multi-directional loss assessment for a curved bridge as a means to identify the impact of seismic incidence angle on its performance for groups of motions with different intensities. Primary conclusions are outlined below:

(1) The performance of an IM with respect to the evaluation criteria depends on the selected EDP. Generally, the combination of spectral accelerations at critical periods ($S_{a,Comb}$) shows the best behavior compared to other IM candidates,which indicates that incorporating the effects of higher modes in defining an IM helps improve the probabilistic demand assessment of curved bridges. Moreover, although PGA is a commonly-used IM, it is not the optimal selection for curved bridges. The same applies to $S_a(T_1)$ given the difficulty to select the direction of the appropriate fundamental period (T_1) to define spectral acceleration.

(2) The direction of seismic excitation does not signifiacantly affect the selection of the optimum IM.

(3) The critical seismic excitation direction of a curved bridge is associated with the earthquake characteristics. Applying the horizontal orthogonal components along the principal axes of curved bridges may significantly underestimate their real seismic loss.

(4) The effect of angle of seismic incidence on the bridge performance weakens as the ground shaking intensity increases. This is because the contribution of higher modes becomes significant as the accumulation of damage throughout the curved bridge dominates the response. Thereby the seismic loss turns out to be direction-independent for strong ground motion intensities.

6. Acknowledgements

This research was supported by the National Natural Science Foundation of China under Grant No. 51778471, 51978512; and the Ministry of Science and Technology of China under Grant No. SLDRCE19-B-19. The second author would also like to thank the the financial support from the China Scholarship Council (CSC) and the University of Bristol for its hospitality during his one year visit.

7. References

[1] Somerville PG (2002): Characterizing near fault ground motion for the design and evaluation of bridges. *3rd National Seismic Conference and Workshop on Bridges and Highways*, Portland, USA.

[2] Jennings PC (1971): Engineering features of the San Fernando earthquake of February 9, 1971. *Technical Report*, California Institute of Technology, Pasadena, USA.

[3] Chandramohan R, Baker JW, Deierlein GG (2013): Influence of ground motion duration on the collapse response of bridge structures. *7th National Seismic Conference on Bridges & Highways*, Oakland, USA.

[4] Stewart JP, Abrahamson NA, Atkinson GM, et al. (2011): Representation of bidirectional ground motions for design spectra in building codes. *Earthquake Spectra*, **27**, 927–37

[5] Taskari O, Sextos A (2015): Multi-angle, multi-damage fragility curves for seismic assessment of bridges. *Earthquake Engineering & Structural Dynamics*, **44**, 2281–2301.

[6] Araújo M, Marques M, Delgado R (2014): Multidirectional pushover analysis for seismic assessment of irregular-in-plan bridges. *Engineering Structures*, **79**, 375–389.

[7] Taskari O, Sextos AG, Kappos AJ (2008): 3D finite element modeling of a highway bridge considering the effect of soil and foundation. *6th GRACM International Congress on Computational Mechanics, Thessaloniki*, Greece.

[8] Feng R, Wang X, Yuan W, Yu J (2018): Impact of seismic excitation direction on the fragility analysis of horizontally curved concrete bridges. *Bulletin of Earthquake Engineering*, **16**, 4705–4733.

[9] Feng R, Lao T, Yuan W, Deng T (2018): A novel method for assessing the critical excitation direction of curved bridges. *IABSE Symposium*, Nantes, France.

[10] Song B, Pan J, Liu Q (2008): Study on critical angle to the seismic response of curved bridges based on pushover method. *14th World Conference on Earthquake Engineering, Beijing*, China.

[11] Moschonas IF, Kappos AJ (2013): Assessment of concrete bridges subjected to ground motion with an arbitrary angle of incidence: static and dynamic approach. *Bulletin of Earthquake Engineering*,**11**, 581-605.

[12] Mander JB, Dhakal RP, Mashiko N, Solberg KM (2007): Incremental dynamic analysis applied to seismic financial risk assessment of bridges. *Engineering Structures*, **29**, 2662–2672.

[13] Kameshwar S, Padgett JE (2017): Characterizing and Predicting Seismic Repair Costs for Bridges. *Journal of Bridge Engineering*, **22**, 1–12.

[14] Ghosh J, Padgett JE (2011): Probabilistic seismic loss assessment of aging bridges using a component-level cost estimation approach. *Earthquake Engineering and Structural Dynamics*, **40**, 1743–1761.

[15] Bradley BA, Cubrinovski M, Dhakal RP, MacRae GA (2010): Probabilistic seismic performance and loss assessment of a bridge–foundation–soil system. *Soil Dynamic and Earthquake Engineering*, **30**, 395–411.

[16] Zhang J, Huo Y (2009): Evaluating effectiveness and optimum design of isolation devices for highway bridges using the fragility function method. *Engineering Structures*, **31**, 1648–1660.

[17] Nielson BG (2005): Analytical fragility curves for highway bridges in moderate seismic zones . *Doctoral dissertation*, Georgia Institute of Technology, Atlanta, USA.

[18] Ramanathan K, DesRoches R, Padgett JE (2012): A comparison of pre- and post-seismic design considerations in moderate seismic zones through the fragility assessment of multispan bridge classes. *Engineering Structures*, **45**, 559–573.

[19] Sextos AG, Kappos AJ, Mergos P (2004): Effect of soil-structure interaction and spatial variability of ground motion on irregular bridges: the case of the Krystallopigi bridge. *13th World Conference on Earthquake Engineering*, Vancouver, Canada.

[20] McKenna F (2011): OpenSees: A framework for earthquake engineering simulation. *Computing in Science & Engineering*, **13**, 58–66.

[21] Mander JB, Priestley MJN, Park R (1988): Theoretical stress-strain model for confined concrete. *Journal of Structural Engineering*, **114**, 1804–26.

[22] Mylonakis G, Nikolaou S, Gazetas G (2006). Footings under seismic loading: Analysis and design issues with emphasis on bridge foundations. *Soil Dynamic and Earthquake Engineering*, **26**, 824–853.

[23] Muthukumar S (2003): A contact element approach with hysteresis damping for the analysis and design of pounding in bridges. *Doctoral dissertation*, Georgia Institute of Technology, Atlanta, USA.

[24] Soleimani F, Vidakovic B, Desroches R, Padgett J (2017). Identification of the significant uncertain parameters in the seismic response of irregular bridges. *Engineering Structures*, **141**, 356–372.

[25] Stefanidou SP, Kappos AJ (2017): Methodology for the development of bridge-specific fragility curves. *Earthquake Engineering and Structural Dynamics*, **46**, 73–93.

[26] Taskari O, Sextos A (2015): Probabilistic Assessment of abutment-embankment stiffness and implications in the predicted performance of short bridges. *Journal of Earthquake Engineering*, **19(5)**, 822–846

[27] Baker JW, Lee C (2017): An improved algorithm for selecting ground motions to match a conditional spectrum. *Journal of Earthquake Engineering*, **22(4)**, 708-723.

[28] Wang X, Shafieezadeh A, Ye A (2018): Optimal intensity measures for probabilistic seismic demand modeling of extended pile-shaft-supported bridges in liquefied and laterally spreading ground. *Bulletin of Earthquake Engineering*, **16**, 229–57.